What Do We Learn from Two-Dimensional Raman Spectra by Varying the Polarization Conditions?

Ao Ma and Richard M. Stratt[*]

Department of Chemistry, Brown University, Providence, RI 02912, USA
Received April 14, 2003

The signals obtained from the 5th-order (two-dimensional) Raman spectrum of a liquid can depend dramatically on the polarizations of the various light beams, but to date there has been no evidence presented that different polarization conditions probe any fundamentally different aspects of liquid dynamics. In order to explore the molecular significance of polarization we have carried out a molecular dynamics simulation of the 5th-order spectrum of a dilute solution of CS_2 in liquid Xe, perhaps the simplest system capable of displaying a full range of polarization dependencies. By focusing on the 5 distinct rotational invariants revealed by the different polarizations and by comparing our results with those from liquid Xe, a liquid whose spectrum has no significant polarization dependence, we discovered that the polarization experiments do, in fact, yield valuable microscopic information. With different linear combinations of the experimental response functions one can separate the part of the signal derived from the purely interaction-induced part of the many-body polarizability from the portion with the largest contributions from single-molecule polarizabilities. This division does not directly address the underlying liquid dynamics, but it significantly simplifies the interpretation of the theoretical calculations which do address this issue. We find that the different linear combinations differ as well in whether they exhibit nodal lines. Despite the absence of nodes with the atomic liquid Xe, observing the resilience of our solution's nodes when we artificially remove the anisotropy of our solute leads us to conclude that there is no direct connection between nodes and specifically molecular degrees of freedom.

Key Words : Liquid, Nonlinear spectroscopy, Two-dimensional spectroscopy, Fifth-order Raman, Molecular dynamics

Introduction

Though to date only one liquid, liquid CS_2, has been persuaded to divulge its two-dimensional (5-th order) Raman spectrum[1-4] in the laboratory,[5-11] neat liquid CS_2 is not necessarily the simplest choice for learning how to interpret such spectra. The same significant polarizability that no doubt contributes to the strength of the experimental signals also mixes the responses from the individual molecular polarizabilities with the more collective responses derived from the various orders of induced polarizabilities.[12-14] Moreover, the fact that the rotations and translations of the CS_2 molecules couple strongly with one another, as well as to the polarizability itself, makes it difficult to ascribe a simple dynamical significance to any of the spectroscopic features.[15]

It was with these considerations in mind that we and a number of other groups decided to begin our analysis of 5-th order Raman spectra by thinking about the spectrum expected from an atomic liquid, liquid Xe.[16-20] The ability to concentrate on purely translational motion and on a single term in the dipole-induced-dipole series[17] meant that we could focus on the more basic question of what the 5-th order signal actually tells us about liquid dynamics. It could have been the case, for example, that the signal arose primarily from nonlinear coupling to the many-body polarizability,[16,17,21] a natural consequence in a nonlinear Raman experiment, but not an especially revealing piece of

information about liquid motion. What we found instead[18] was that it was largely the intrinsic anharmonicity of the molecular dynamics that generated the signal in this example.[22-24] We found, in addition, that this anharmonicity was surprisingly weak: it was amply capable of causing pure dephasing of the liquid's instantaneous normal modes, but it seemed to be insufficient to destroy the essentially harmonic definitions of the modes.[18]

Of course, an atomic liquid is a rather special case. Atoms have neither the possibility of an anisotropic polarizability nor the opportunity to undergo rotational motion. To help us learn about the kinds of effects that we might expect to see in a specifically molecular liquid -- without bringing in all of the potential complications -- we therefore decided to examine the simplest step up from an atomic liquid: an infinitely dilute solution of CS_2 dissolved in liquid Xe.[25] What makes this case particularly straightforward is that the molecular polarizability of CS_2 is sufficiently larger than that of Xe

$$\ddot{\alpha}(CS_2) = \alpha(CS_2)\,\ddot{I} + \frac{2}{3}\gamma(CS_2)\,\ddot{Q}, \qquad (1)$$

$$\ddot{Q} = \frac{3}{2}\mathbf{ee} - \frac{1}{2}\ddot{I}, $$

$$\ddot{\alpha}(Xe) = \alpha(Xe)\,\ddot{I}, \qquad (2)$$

where $\alpha(CS_2)$ = 8.95 Å^3 and $\gamma(CS_2)$ = 10.05 Å^3 are the isotropic and anisotropic components of CS_2's polarizability,[13] $\alpha(Xe)$ = 4.11 Å^3 is the isotropic (and only) component of

Xe's polarizability,[26] and **e** is a unit vector directed along the CS_2 bonding axis, that the many-body polarizability of the solution Π is well approximated by the sum of the molecular polarizability of the CS_2 and the leading term in the induced polarizability.[13,17]

$$\ddot{\Pi} = \ddot{\alpha}(CS_2) + \ddot{\Pi}_{induced} , \qquad (3)$$

$$\ddot{\Pi}_{induced} = \ddot{\alpha}(CS_2) \bullet \sum_{j=1}^{N} \ddot{T}(\mathbf{r}_{0j}) \bullet \ddot{\alpha}(Xe)$$

$$+ \ddot{\alpha}(Xe) \bullet \sum_{j=1}^{N} \ddot{T}(\mathbf{r}_{0j}) \bullet \ddot{\alpha}(CS_2). \qquad (4)$$

Here, the center of mass of the CS_2 molecule is assumed to be located at $\mathbf{r}_0$, the sums are over the Xe solvent atoms located at $\mathbf{r}_j = \mathbf{r}_0 - \mathbf{r}_{0j}$ ($j = 1, \ldots, N$), and the dipole-dipole tensor is defined to be $\ddot{T}(\mathbf{r}) = (3\hat{r}\hat{r} - \ddot{1})/r^3$.

The fifth-order signal itself is still an involved function of this polarizability. In its most basic form, the experiment involves subjecting the sample to two pairs of visible light pulses separated by a time interval t_1, followed by a measurement of the light scattering from a fifth visible pulse a time t_2 later.[1-3] In the limit of purely classical motion, the response function for this scattering can be written as an ensemble average[16,17,21,27]

$$R^{(5)}(t_1, t_2) = \langle \{\{\ddot{\Pi}(t_1 + t_2), \ddot{\Pi}(t_1)\}, \ddot{\Pi}(0)\} \rangle , \qquad (5)$$

involving the Poisson brackets of the many-body polarizability evaluated at the three different times relevant to the experiment. If the coordinates and momenta of the species in the liquid are designated as $r_{j\mu}$ and $p_{j\mu}$ respectively, with $j = 0$ referring to the sole CS_2 molecule, and μ denoting all of the intramolecular coordinates (x, y, and z for each Xe and for the CS_2 center of mass along with the orientational coordinates for CS_2), then the Poisson brackets we need are of the form

$$\{A(t), B(t')\} =$$

$$\sum_{j=0}^{N} \sum_{\mu} \left[\frac{\partial A(t)}{\partial r_{j\mu}(0)} \frac{\partial B(t')}{\partial p_{j\mu}(0)} - \frac{\partial A(t)}{\partial p_{j\mu}(0)} \frac{\partial B(t')}{\partial r_{j\mu}(0)} \right]. \qquad (6)$$

Thus the experiment examines a kind of second-order sensitivity of the polarizability to perturbations of the initial conditions, $(\mathbf{r}_j(0), \mathbf{p}_j(0))$.[17]

Although introducing molecules to our liquid does add a level of complexity to this already complex scenario, a feature of molecular liquids that more than counterbalances any difficulties is that the presence of anisotropic molecules affords us an additional experimental handle: the choice of polarization conditions.[28-30] As one might expect from the fact that the response function, Eq. (5), depends on 6 different tensor indices (two for each appearance of $\ddot{\Pi}$), the fifth-order Raman spectrum of neat liquid CS_2 exhibits a dramatic dependence on polarization conditions.[6,8,31,32] Just what molecular interpretation one should place on this dependence, though, has never been clear. The first goal of

the present work is therefore to see if examining our conceptually simpler mixed system can help us understand the different dynamical signatures of the various polarizations.

Once we are armed with such results, there are other aspects of the CS_2 experiments that we should be able to consider. A consistent prediction from both Xe and CS_2 molecular dynamics simulations is a ridge along the t_2 axis ($t_1 = 0$).[17,31,32] Although an unambiguous experimental observation is awkward because of hyperpolarizability and finite-pulse-duration effects,[6,7,33] it has been pointed out that this region is conceptually intriguing. If we think of the liquid's ultrafast dynamics as a superposition of various intermolecular vibrations, the suggestion is that we should regard measurements along this axis as a direct measurement of vibrational population relaxation.[6,19,21,34] Indeed, WKB instantaneous-normal-mode calculations on Xe − which allow for pure dephasing but manifestly omit such energy relaxation mechanisms − exhibit a strikingly prolonged response along this axis.[18] Our current work should allow us to see how universal this t_2 ridge phenomenon is and, to the extent the behavior is universal, to see which molecular degrees of freedom contribute to it the most.

The other noteworthy feature of the most recent experimental and theoretical studies of neat liquid CS_2 is the presence of nodal lines − lines in the (t_1, t_2) plane where the response function changes sign.[8,31] Since calculations on Xe, an atomic liquid, do not show any such nodal lines,[17] it is possible that these nodes signify something uniquely molecular about the dynamics or the coupling. But it is also conceivable that it is the relatively low polarizability of Xe (which makes the leading term in its dipole-induced-dipole series so dominant) that suppresses the nodes − and that some other atomic liquid could, in principle, have nodal lines. Here again, the ability to examine the CS_2/Xe mixture gives us a chance to gain some insight into the molecular origins of the spectra.

This paper, then, will present the results of a molecular dynamics simulation of the 5-th-order Raman response for CS_2 dissolved in liquid Xe. Section II sets out the details of the model, the precise form of the response functions we compute, and the algorithm required to propagate our Poisson brackets. The results from our simulation are described in Sec. III, and we conclude in Sec. IV with a summary of what one can and cannot discern from such a simulation. A future publication will round out the picture by presenting the results of a traditional and an anharmonically corrected instantaneous-normal-mode analysis performed on this same system.[35]

The Simulation Model and Methods

The model we consider consists of a single rigid CS_2 molecule, regarded as three collinear Lennard-Jones atoms, and 29 Xe atoms, also taken to interact via Lennard-Jones potentials. The parameters used are standard ones for CS_2 and Xe along with those from the standard Lorentz-Berthelot combining rules for the CS_2/Xe interactions (Table 1).[13,36,37] The system was equilibrated at a reduced density of

1128 *Bull. Korean Chem. Soc.* **2003**, Vol. 24, No. 8

Ao Ma and Richard M. Stratt

Table 1. Model parameters for our simulation of CS_2 in liquid Xe[a]

Atom	σ (Å)[b]	ε/k_B (K)[b]	m (amu)[c]
C	3.35	51.2	12.01
S	3.52	183.0	32.06
Xe	4.099	222.3	131.3

[a]The potential energy of the system consists of a sum of Xe-Xe pair potentials $u_{XeXe}(r)$ plus a Xe-X pair potential $u_{XeX}(r)$ for each atom X = S, C or S in CS_2. The pair potentials between atoms of species A and species B are given by $u_{AB}(r) = 4\varepsilon_{AB}[(\sigma_{AB}/r)^{12}-(\sigma_{AB}/r)^6)]$. The C-S distance in CS_2 is fixed at 1.57 Å. [b]Lennard-Jones parameters for atoms interacting with other atoms of the same kind (*i.e.*, for an atom of species A, $\sigma = \sigma_{AA}$, $\varepsilon = \varepsilon_{AA}$). For interactions between atoms of species A and B, we use the values $\sigma_{AB} = 1/2(\sigma_A + \sigma_B)$ and $\varepsilon_{AB} = \sqrt{\varepsilon_A \varepsilon_B}$. [c]Atomic mass.

$\rho\sigma_{XeXe}^3 = 0.8$ and a reduced temperature $k_B T/\varepsilon_{XeXe} = 1.0$, well within the liquid range, and we carried out an NVE simulation to trace the time evolution of the many-body polarizability (which was specified as we indicated in the previous section). The specifics of calculating the 5th order spectrum are described in more detail below.

A. The response function and its tensor invariants. Although we could, in principle, base our calculations on the formal expression for the classical 5th order response function shown in Eq. (5), we can avoid having to compute a nested set of Poisson brackets by transforming the ensemble-averaged expression so that it involves just a single Poisson bracket. The transformation we use here is one derived in an earlier paper[17]

$$R^{(5)}(t_1,t_2) = \beta\langle\dot{\ddot{\Pi}}(0)\{\ddot{\Pi}(t_1), \ddot{\Pi}(t_1+t_2)\}\rangle$$

$$= \beta\langle\dot{\ddot{\Pi}}(-t_1)\{\ddot{\Pi}(0), \ddot{\Pi}(t_2)\}\rangle, \qquad (7)$$

a version particularly well-suited to numerical calculation in that it avoids computing small differences between averaged quantities. Here $\beta = (k_B T)^{-1}$.

Evaluating the remaining Poisson bracket still requires that we look at the time evolution of the derivatives of the many-body polarizability with respect to initial conditions, Eq. (6), a process that can produce numerically awkward divergences if we regard the CS_2 orientation angles θ and ϕ as being among the time evolving coordinates. However the problem can be removed simply by propagating the three Cartesian components of the CS_2 orientation unit vector **e** rather than propagating θ and ϕ. It is therefore convenient to be able to express the Poisson bracket in terms of both the $3N+5$ original initial coordinates $r_{j\mu}(0)$ and a new set of $3N+6$ coordinates at time t, $R_{k\chi}(t)$. As before we take $j, k = 0, \ldots, N$ to label the solute and solvent molecules, and we use $\mu = \chi = x, y$ or z for the solute center-of-mass and solvent coordinates, but instead of having the solute orientational coordinates be just $r_{0\mu} = \theta, \phi$, we characterize the orientation by $R_{0\chi} = e_x, e_y, e_z$. In particular, using the chain rule we write

$$\{\ddot{\Pi}(0), \ddot{\Pi}(t)\} = \sum_{j,k=0}^{N}\sum_{\mu,\chi} \ddot{\Pi}_{j\mu}(0)\ddot{\Pi}_{k\chi}(t)J_{k\chi,j\mu}^{Rp}(t)$$

$$\ddot{\Pi}_{j\mu}(0) = \partial\ddot{\Pi}(0)/\partial r_{j\mu}(0), \quad \ddot{\Pi}_{k\chi}(t) = \partial\ddot{\Pi}(t)/\partial R_{k\chi}(t),$$
$$(8)$$

which expresses the polarizability dynamics in terms of a *fundamental* Poisson bracket, the Jacobian[17]

$$J_{k\chi,j\mu}^{Rp}(t) = \partial R_{k\chi}(t)/\partial p_{j\mu}(0), \qquad (9)$$

where we have adopted the definitions

$$r_{j\mu}, p_{j\mu} = \begin{cases} (\mathbf{r}_0)_\mu, & M(\dot{\mathbf{r}}_0)_\mu & (j=0, \ \mu=x,y,z) \\ \theta, & I\dot{\theta} & (j=0, \ \mu=\theta) \\ \phi, & I\sin^2\theta\dot{\phi} & (j=0, \ \mu=\phi) \\ (\mathbf{r}_j)_\mu, & m(\dot{\mathbf{r}}_j)_\mu & (j\neq 0, \ \mu=x,y,z) \end{cases} \quad (10)$$

The other issue mitigating against doing our calculations using Eq. (5) as it is written concerns the 6 unspecified tensor indices $(a, b, c, d, e, f) = x, y$ or z. There are, in fact, only 5 rotationally invariant combinations of the $R_{abcdef}^{(5)}$ response functions: The only rotationally invariant combinations of the many-body polarizability tensors at three different times involve the trace (Tr), pair product (PP), and triple product (TP):[28,29]

$$\text{Tr}(\ddot{\Pi}(t)) = \sum_a \Pi_{aa}(t)$$

$$\text{PP}(\ddot{\Pi}(t), \ddot{\Pi}(t')) = \sum_{a,b} \Pi_{ab}(t)\Pi_{ab}(t')$$

$$\text{TP}(\ddot{\Pi}(t), \ddot{\Pi}(t'), \ddot{\Pi}(t'')) = \sum_{a,b,c} \Pi_{ab}(t)\Pi_{ac}(t')\Pi_{bc}(t'').$$
$$(11)$$

So, the only rotationally invariant observables stemming from Eq. (5) (or for that matter, from Eq. (7)) are of the form

$$\text{TP}(0, 1, 2) \equiv \text{TP}(\ddot{\Pi}(0), \ddot{\Pi}(t_1), \ddot{\Pi}(t_1+t_2))$$

$$\text{PP}(0, 1)\, \text{T}(2) \equiv \text{PP}(\ddot{\Pi}(0), \ddot{\Pi}(t_1))\, \text{Tr}(\ddot{\Pi}(t_1+t_2))$$

$$\text{PP}(1,2)\, \text{T}(0) \equiv \text{PP}(\ddot{\Pi}(t_1), \ddot{\Pi}(t_1+t_2))\, \text{Tr}(\ddot{\Pi}(0))$$

$$\text{PP}(0, 2)\, \text{T}(1) \equiv \text{PP}(\ddot{\Pi}(0), \ddot{\Pi}(t_1+t_2))\, \text{Tr}(\ddot{\Pi}(t_1))$$

$$\text{T}(0)\, \text{T}(1)\, \text{T}(2) \equiv \text{Tr}(\ddot{\Pi}(0))\, \text{Tr}(\ddot{\Pi}(t_1))\, \text{Tr}(\ddot{\Pi}(t_1+t_2)). \quad (12)$$

The actual calculations of Eq. (7) are therefore performed for just these 5 invariants. Results for specific experimental polarizations (such as abcdef = zzzzzz) can then be computed from simple linear combinations of the invariants.[28] Aside from minimizing the redundancy of the calculations, we have shown in our previous work that this kind of approach has the side benefit of providing a valuable extra measure of averaging for the computed signals.[16,17]

B. Evaluating the fundamental Poisson bracket. The equations of motion for the fundamental Poisson bracket are most easily derived from the second derivative of Eq. (9)

$$\dot{J}_{k\chi,j\mu}^{Rp}(t) = \partial\ddot{R}_{k\chi}(t)/\partial p_{j\mu}(0), \qquad (13)$$

which, itself, can be written in terms of the time-dependent dynamical matrix (the Hessian of the potential energy V)

$$D_{k\chi,k'\chi'}(t) = \partial^2 V / \partial R_{k\chi} \partial R_{k'\chi'}. \qquad (14)$$

For translational components χ, the equations of motion are simply

$$\ddot{J}^{Rp}_{i\chi,k\mu}(t) = -\frac{1}{m_i}\sum_{j,\chi'} D_{i\chi,j\chi'}(t) J^{Rp}_{j\chi',k\mu}(t) \ (\chi=x,y,z). \quad (15)$$

where m_i is the mass of molecule i, and the index χ' runs over all $3N+6$ of our translational and rotational coordinates.

A more compact notation arises by labeling the $3N+6$ dimensional vectors with arrows $(\vec{R})$, $3N+5$ dimensional vectors with tildes $(\tilde{r})$, and matrices by the appropriate pairs of these labels. If we define the $(3N+6) \times (3N+6)$ molecular mass matrix $\underset{\Rightarrow}{M}$, for example, by

$$(\underset{\Rightarrow}{M})_{j\chi,k\chi'} = \begin{cases} m_j \delta_{j,k}\delta_{\chi,\chi'} & , \chi,\chi' = x,y,z \\ I\delta_{j,0}\delta_{k,0}\delta_{\chi,\chi'} & , \chi \text{ or } \chi' \neq x,y,z \end{cases}, \qquad (16)$$

and define the elements of the Jacobian $(\underset{\Rightarrow}{J})$ and dynamical $(\underset{\Rightarrow}{D})$ matrices by Eqs. (13) and (14), then Eq. (15) can be written

$$\underset{\sim}{\ddot{J}}^{Rp}(t)_{trans} = -\left[\underset{\Rightarrow}{M}^{-1}\right]_{trans} \bullet \underset{\Rightarrow}{D}(t) \bullet \underset{\sim}{J}^{Rp}(t), \qquad (17)$$

where the subscript "trans" refers to the $(3N+3) \times (3N+6)$ matrix containing just the translational (row) components.

However the dynamics of the rotational components of the Poisson bracket, $\chi = e_x, e_y, e_z$ are somewhat more involved because the equation of motion for the rotational coordinates themselves are a bit more complicated. Denoting 3-vectors by boldface characters, we can express the rotational dynamics of our linear solute $\mathbf{e}(t)$ in terms of the torque $\mathbf{g}$ and the moment of inertia I,[38,39]

$$\ddot{\mathbf{e}} = \frac{1}{I}(\vec{1} - \mathbf{ee}) \bullet \mathbf{g} - (\dot{\mathbf{e}}\bullet\dot{\mathbf{e}})\mathbf{e}, \ \ \mathbf{g} = -\frac{\partial V}{\partial \mathbf{e}}. \qquad (18)$$

Since the derivatives with respect to initial momenta involve the rotational (row) components of the Jacobian and dynamical matrices

$$\frac{\partial \mathbf{g}(t)}{\partial \underset{\sim}{p}(0)} = -\underset{\Rightarrow}{D}(t)_{rot} \bullet \underset{\sim}{J}^{Rp}(t)$$

$$\frac{\partial \mathbf{e}(t)}{\partial \underset{\sim}{p}(0)} = \underset{\sim}{J}^{Rp}(t)_{rot}, \ \frac{\partial \dot{\mathbf{e}}(t)}{\partial \underset{\sim}{p}(0)} = \underset{\sim}{\dot{J}}^{Rp}(t)_{rot}, \qquad (19)$$

the equivalent to Eq. (17) for the rotational (row) components of our Poisson bracket becomes

$$\underset{\sim}{\ddot{J}}^{Rp}(t)_{rot} = -\frac{1}{I}(\vec{1} - \mathbf{ee}) \bullet \underset{\Rightarrow}{D}(t)_{rot} \bullet \underset{\sim}{J}^{Rp}(t)$$

$$-\frac{1}{I}\mathbf{g}(t) \bullet \left[\mathbf{e}(t)\underset{\sim}{J}^{Rp}(t)_{rot} + \underset{\sim}{J}^{Rp}(t)_{rot}\mathbf{e}(t)\right]$$

$$-\left[\dot{\mathbf{e}}(t)\bullet\dot{\mathbf{e}}(t)\right]\underset{\sim}{J}^{Rp}(t)_{rot} - 2\left[\underset{\sim}{\dot{J}}^{Rp}(t)_{rot}\bullet\dot{\mathbf{e}}(t)\right]\mathbf{e}(t). \qquad (20)$$

Equations of motions such as those of Eq. (17) lend themselves naturally to numerical solution by conventional

molecular dynamics algorithms. In schematic terms, since $\underset{\Rightarrow}{D}(t) = \underset{\Rightarrow}{D}[\vec{R}(t)]$, this equation has the form of a simple 2nd order differential equation for a matrix $\underset{\bullet\bullet}{J}(t)$

$$\underset{\bullet\bullet}{\ddot{J}}(t) = \underset{\bullet\bullet}{F}\left[\underset{\bullet\bullet}{J}(t); \underset{\rightarrow}{R}(t), \underset{\rightarrow}{\dot{R}}(t)\right], \qquad (21)$$

coupled to the trajectory $\vec{R}(t)$ of our liquid. Hence we can propagate the elements of $\underset{\bullet\bullet}{J}(t)$ with time step δ, just by using the central difference (Verlet) algorithm[39]

$$\underset{\bullet\bullet}{J}(t+\delta) = 2\underset{\bullet\bullet}{J}(t) - \underset{\bullet\bullet}{J}(t-\delta) + \delta^2\underset{\bullet\bullet}{F}(t),$$

$$\underset{\bullet\bullet}{F}(t) \equiv \underset{\bullet\bullet}{F}\left[\underset{\bullet\bullet}{J}(t); \underset{\rightarrow}{R}(t), \underset{\rightarrow}{\dot{R}}(t)\right]. \qquad (22)$$

The corresponding rotational component equations of motion, Eq. (20), are of a slightly different form

$$\underset{\bullet\bullet}{\ddot{J}}(t) = \underset{\bullet\bullet}{G}\left[\underset{\bullet\bullet}{J}(t); \underset{\rightarrow}{R}(t), \underset{\rightarrow}{\dot{R}}(t)\right] + \underset{\bullet\bullet}{M}\left[\underset{\rightarrow}{R}(t), \underset{\rightarrow}{\dot{R}}(t)\right] \bullet \underset{\bullet\bullet}{\dot{J}}(t). \ (23)$$

but if we express both the "velocity" and the "acceleration" in central difference form

$$\underset{\bullet\bullet}{\dot{J}}(t) = \frac{1}{2\delta}\left[\underset{\bullet\bullet}{J}(t+\delta) - \underset{\bullet\bullet}{J}(t-\delta)\right]$$

$$\underset{\bullet\bullet}{\ddot{J}}(t) = \frac{1}{\delta^2}\left[\underset{\bullet\bullet}{J}(t+\delta) - 2\underset{\bullet\bullet}{J}(t) + \underset{\bullet\bullet}{J}(t-\delta)\right],$$

we find that we can propagate Eq. (23) in much the same fashion

$$\underset{\bullet\bullet}{J}(t+\delta) = \left(\underset{\bullet\bullet}{1} - \frac{\delta}{2}\underset{\bullet\bullet}{M}(t)\right)^{-1}$$

$$\bullet \left[2\underset{\bullet\bullet}{J}(t) - \left(\underset{\bullet\bullet}{1} + \frac{\delta}{2}\underset{\bullet\bullet}{M}(t)\right)\underset{\bullet\bullet}{J}(t-\delta) + \delta^2\underset{\bullet\bullet}{G}(t)\right]. \qquad (24)$$

Moreover for us, the 3×3 matrix $\underset{\bullet\bullet}{M} = -2\mathbf{e\dot{e}}$. Since $\dot{\mathbf{e}} \bullet \mathbf{e} = 0$,

$$\underset{\bullet\bullet}{M} \bullet \underset{\bullet\bullet}{M} = \underset{\bullet\bullet}{M} \bullet \underset{\bullet\bullet}{M} \bullet \underset{\bullet\bullet}{M} = \cdots = 0,$$

so the terms involving $\underset{\bullet\bullet}{M}$ are just

$$\left(\underset{\bullet\bullet}{1} - \frac{\delta}{2}\underset{\bullet\bullet}{M}(t)\right)^{-1} = \left(\underset{\bullet\bullet}{1} + \frac{\delta}{2}\underset{\bullet\bullet}{M}(t)\right) = \underset{\bullet\bullet}{1} - \delta\mathbf{e}(t)\dot{\mathbf{e}}(t). \quad (25)$$

Both portions of the $\underset{\sim}{J}^{Rp}(t)$ trajectory can now be launched simply by using the initial conditions. Since $\underset{\sim}{J}^{Rp}(0) = \underset{\Rightarrow}{0}$ and it is easy to find $\underset{\sim}{\dot{J}}^{Rp}(0)$, we can initiate both Eqs. (22) and (24) by making use of the expresssion

$$\underset{\sim}{J}^{Rp}(-\delta) = -\delta\underset{\sim}{\dot{J}}^{Rp}(0) + \frac{1}{2}\delta^2\underset{\sim}{\ddot{J}}^{Rp}(0), \qquad (26)$$

$$\left[\underset{\sim}{\dot{J}}^{Rp}(0)\right]_{j\chi,k\mu} = \left[\underset{\Rightarrow}{M}^{-1}\right]_{j\chi,k\chi}\delta_{\chi,\mu} \ , \quad (\chi=x,y,z)$$

$$\left[\underset{\sim}{\ddot{J}}^{Rp}(0)\right]_{j\chi,k\mu} = 0 \qquad\qquad , \quad (\chi=x,y,z)$$

$$\left[\underset{\sim}{\dot{J}}^{Rp}(0)\right]_{j\chi,k\mu} = \delta_{j,0}\delta_{k,0}\frac{\partial\dot{e}_\chi(0)}{\partial p_\mu(0)} \ , \quad (\chi \neq x,y,z)$$

$$\left[\underset{\sim}{\ddot{J}}^{Rp}(0)\right]_{j\chi,k\mu} = -2\left[\underset{\sim}{\dot{J}}^{Rp}(0)_{rot} \bullet \dot{\mathbf{e}}(0)\right]\mathbf{e}(0), \ (\chi \neq x,y,z)$$

where the values of the second time derivatives follow from Eqs. (17) and (20).

Parenthetically, we should also point out that while this scheme for propagating the Jacobian is free of the divergences we alluded to earlier -- divergences triggered by $\theta(t)$ passing near 0 or π during the course of the trajectory -- these special values can still lead to divergences at the start of the trajectory. Such problems can be avoided by transforming the coordinate system used to define **e**

$$\mathbf{e} = (\sin\theta\cos\phi,\ \sin\theta\sin\phi,\ \cos\theta) \rightarrow$$
$$\mathbf{e} = (\cos\theta',\ \sin\theta'\sin\phi',\ \sin\theta'\cos\phi')$$

whenever the initial angle θ is near 0 or π.[40]

C. Computational details. The dynamics of the solution itself was simulated in conjunction with that of the fundamental Poisson bracket by using the velocity Verlet algorithm for solute and solvent translation and the Rattle algorithm to describe the solute rotation.[39,41,42] All the simulations employed a time step of $\delta = 0.001\ \tau_{LJ}(Xe) = 3.47$ fs, with the initial liquid structure equilibrated for 10^4 time steps from a zero-translational-order-parameter[43] liquid configuration before taking any data.

All response functions reported here were averaged over 10^6 statistically independent liquid configurations.

Results

We begin our presentation by looking at the variety of 5th-order responses that we can obtain from our solution, Figure 1.

Just as in the neat liquid CS_2, changing polarization conditions for our simpler system does indeed produce some noticeable changes in the response functions.[6,8,31,32] The all-parallel (zzzzzz) polarization yields a kidney shape quite similar to that found with neat liquid Xe,[16,17] but with a peak at ($t_1 \approx 140$ fs, $t_2 \approx 170$ fs), much closer to the $t_1 = t_2$ echo line than we saw in pure Xe ($t_1 \approx 30$ fs, $t_2 \approx 330$ fs). Rotating the final two polarizations to the magic angle (resulting in the mmzzzz polarization) generates a peak and a lengthy ridge along the t_2 axis, with a distinct, mostly vertical, nodal line near $t_1 = 200$-250 fs, and an overall shape remarkably similar to that seen in Saito and Ohmine's simulation of the mmzzzz response for neat liquid CS_2 (despite the absence of a node in the latter).[31] The yyzzzz polarization shows yet another set of motifs. The t_2 ridge and the associated node are now combined with valley along the echo direction featuring a minimum at ($t_1 \approx 200$ fs, $t_2 \approx 210$ fs).

The diversity of these plots not withstanding, the most fundamental results from this study are not going to be these spectra, but the five rotational invariants described by Eq. (12). We therefore turn in Figure 2 to the response functions appropriate for each of these.

As this figure makes quite clear, the reason that different polarization conditions give rise to such different spectra is that the invariants from which they are constructed are so markedly different. Both of the invariants involving T(2) (the trace of the polarizability at time $t_1 + t_2$) have an extended
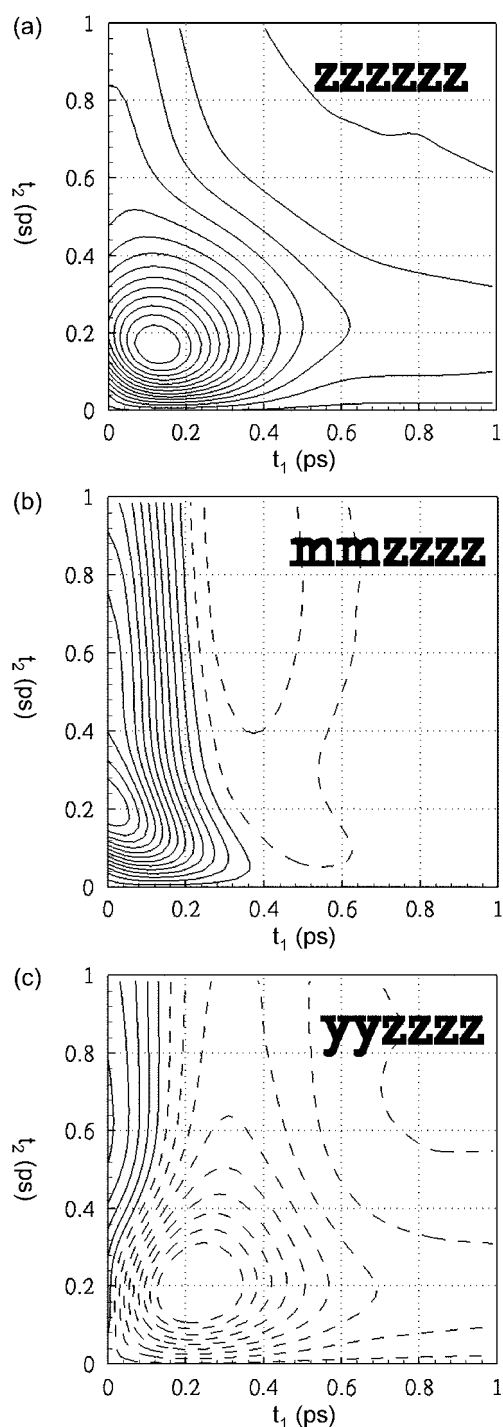

Figure 1. Molecular dynamics simulations of the 5th-order Raman response functions $R_{abcdef}^{(5)}(t_1, t_2)$ for an infinitely dilute solution of CS_2 in liquid Xe. The three panels display the results for three different choices of polarization conditions (the tensor indices a, b, c, d, e, f); "m" denotes the magic angle. Contour plots shown in this and all succeeding figures have 15 equally spaced contours between the minimum and maximum values, with negative values indicated by dashed lines.

ridge along the t_2 axis. By contrast, the TP invariant (the one involving the triple product of the polarizability at the times 0, t_1, and $t_1 + t_2$) and the PP(0, 2) T(1) invariant both have a sharp peak located a short distance along the echo ($t_1 = t_2$)
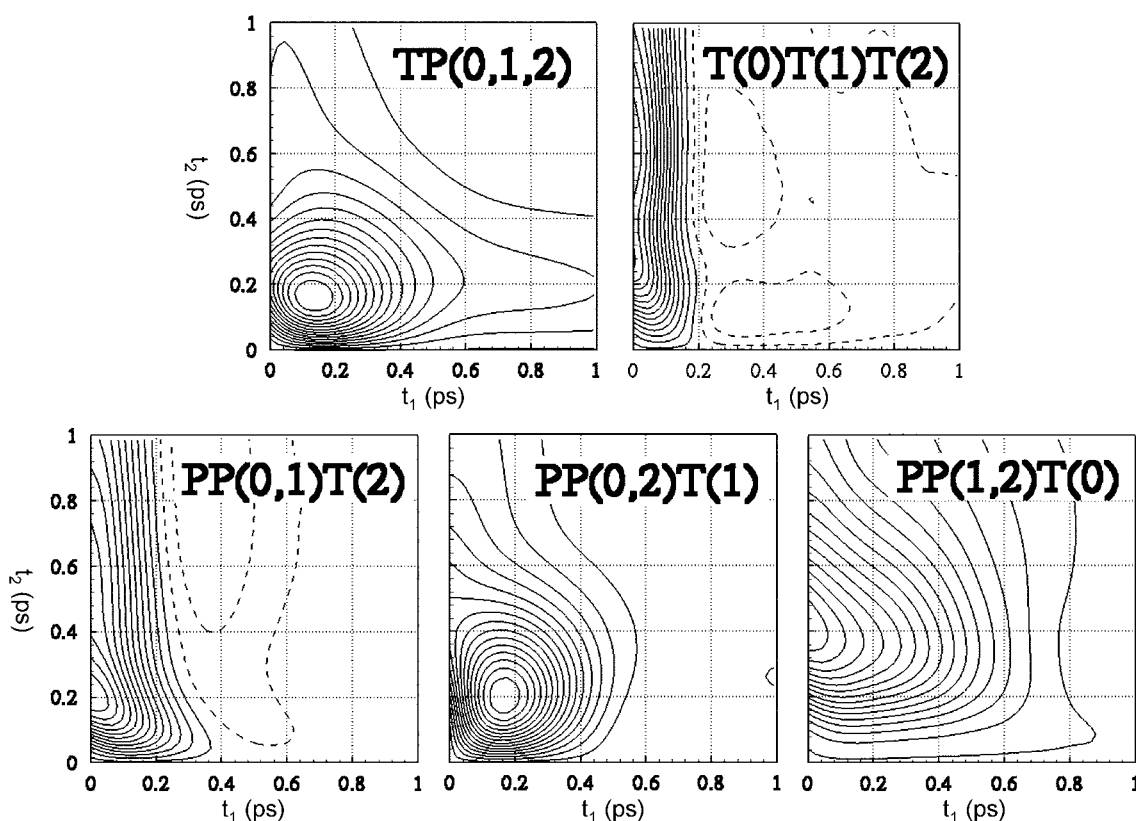
Figure 2. Molecular dynamics simulation results for the five different rotational invariants entering into the 5th-order Raman signal for our solution of CS_2 in liquid Xe. In our notation (0, 1, 2) refers to the many-body polarizabilities at times 0, t_1 and $t_1 + t_2$, respectively, T refers to a trace, PP to a pair-product over two of the polarizabilities, and TP to a triple product over all three of the polarizabilities. The explicit connections between these invariants and the response functions shown in Fig. 1 are detailed in Table 2.

diagonal. The remaining invariant PP(1, 2) T(0) is different still; it has a much broader peak located directly on the t_2 axis. Of course, the other intriguing feature of these invariants has to do with the presence of nodal lines. Out of all the invariants, we note that only those involving T(2) display these nodes.

So what distinguishes these invariants physically? Looking back at Eqs. (3) and (4) tells us that the many-body polarizability at each time is the sum of a contribution from the CS_2 solute itself, $\ddot{\Pi}_{mol} = \ddot{\alpha}(CS_2)$ − a tensor which is fixed in the molecular frame and whose dynamics can therefore *only* arise from CS_2 reorientation − and an interaction-induced term $\ddot{\Pi}_{induced}$ − which will evolve whenever either the CS_2 rotates or the solute-solvent center of mass distance changes. The trace of $\ddot{\Pi}_{mol}$, though, cannot

Table 2. Response function for different choices of polarization conditions[a]

c	T(0)T(1)T(2)	PP(0,1)T(2)	PP(0,2)T(1)	PP(1,2)T(0)	TP(0,1,2)
z	1/105	2/105	2/105	2/105	8/105
m	1/15	2/15	0	0	0
y	1/35	2/35	−1/105	−1/105	−4/105

[a]The contributions of each of the 5 rotational invariants to the 5th-order Raman response function $R^{(5)}_{cczzzz}(t_1, t_2)$ for different choices of the final $(t_1 + t_2)$ polarization "c". Here "m" denotes the magic angle. Adopted from refs. 28, 29.

evolve at all; it is fixed at $3\alpha(CS_2) = 3(8.95)$ Å[3]. The end result is that any invariant involving the trace of a single many-body polarizability at some time t looks only at the induced portion of the polarizability, at least at that time.[44] The most extreme example, the triple-trace invariant T(0)T(1)T(2), sees nothing but interaction-induced contributions to the 5th order spectrum. As a consequence, the numerical contribution of this invariant is far smaller than that of any of the other invariants (and, in fact, may be safely neglected for our system).

Given this analysis it is hardly surprising that the invariant that contributes the most to the overall spectrum is the triple product, TP(0, 1, 2) (the one without any traces over individual polarizabilities). Quite generally, whenever the substantial dynamics of the purely molecular polarizability, $\ddot{\Pi}_{mol}(t)$, is not hidden by symmetry considerations, we expect it to dominate the spectrum of our solution.[45] We can confirm this expectation quite simply by partitioning the triple-product spectrum into the component coming from the solely molecular terms, the component stemming from the purely interaction-induced terms, and the cross terms, Figure 3. Despite the fact that the latter two contributions outnumber the pure molecular term 7 to 1, the former − which represents purely rotational dynamics − accounts for 75% of the total triple-product response.

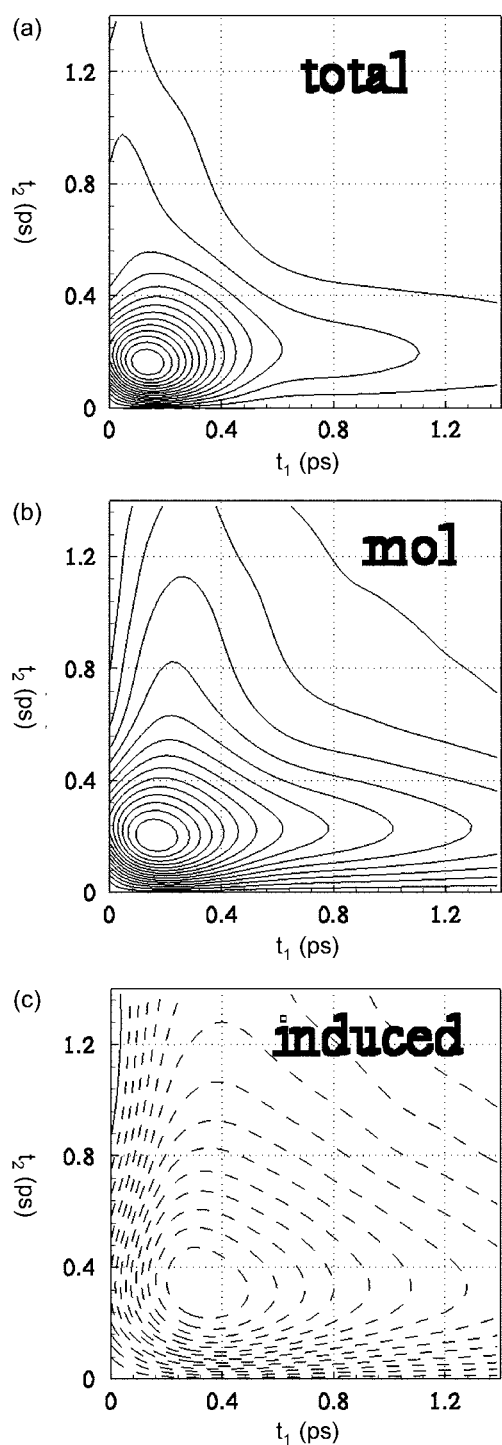The physical importance of these observations is that we

Figure 3. Contributions to the TP invariant for our solution of CS_2 in liquid Xe. (a) Molecular dynamics simulation of the complete invariant. (b) The contribution from purely single-molecule polarizabilities. (c) The contribution from the purely interaction-induced components. Contributions from the remaining single-molecule/interaction-induced cross terms are not shown.

can now begin to point to the 5th-order Raman signatures of various contributions to the dynamics. Pure reorientational motion evidently shows up in this system as a sharp peak located about 150 fs along the echo diagonal with crescent-shaped wings appearing symmetrically along both the t_1 and

t_2 axes. We know the precise appearance of the interaction-induced part of the 5th-order spectrum as well. But it is worth remembering that this last information is not necessarily a help in interpreting the underlying molecular motions. The label "interaction-induced" refers to a component of the coupling of the system to the spectroscopic signal; it does not, in itself, imply any kind of dynamical characterization. Indeed, as we have mentioned, both rotation and translation could contribute to its time evolution in this example. Nonetheless it may be significant that this spectrum has a noticeable asymmetry, with almost all of the response concentrated near the t_2 axis. This same motif shows up in anharmonic instantaneous-normal-mode treatments of neat liquid Xe.[18] Since these treatments allow for dephasing of effectively independent dynamical degrees of freedom, but ignore the possibility of dynamical mode-mode coupling, the interaction-induced portion of our solution spectrum may very well be reporting on the component of the dynamics that displays an independent-mode behavior.[18,19]

Interestingly, these same figures also place us in a position to say something about the significance of nodal lines. Although it is hard to see on the scale of the figure, and despite the fact that the full triple-product invariant does not exhibit a node, the induced portion of this invariant actually has a nodal line close to the t_2 axis. Perhaps the most important conclusion to draw from this fact is that nodes are subtle. The presence of a node in one spectrum and the absence in another might not be all that physically significant. Nodes might simply appear and disappear with small shifts in the delicate cancellations among the various contributions to the spectrum.

We can elaborate on this point by looking in a little more detail at the relationship between our solution and neat liquid Xe. The same triple product is the only nonzero tensor invariant for the 5th-order Raman spectrum of neat liquid Xe (through the leading order in the dipole-induced-dipole series) and the entire Xe spectrum is interaction-induced.[17] This spectrum, however, does not have any nodal lines. Is there something about the difference between an atomic liquid and a molecule dissolved in an atomic liquid that generates a node in the latter but not in the former?

It is easy enough to examine each of the possible distinctions between these examples, Figure 4. Molecules have anisotropic intermolecular interactions, which affects the liquids structure and dynamics, as well as an anistropic polarizability, which influences the coupling of that dynamics to the spectroscopic response. Suppose we simply turn off the polarizability anisotropy of our solute. When we do so (Fig. 4a), we find that the interaction-induced part of the triple-product invariant has an even more pronounced node. If we then make this artificial CS_2 solute even more atom-like by making the potential nearly isotropic, say by shrinking the C-S distance to 1% of its physical value (Fig. 4b), we find that the node still remains robust.

At this point, though, we have erased all the molecular features of our solute. The lack of polarizability anisotropy means that the solute's orientation can no longer have any
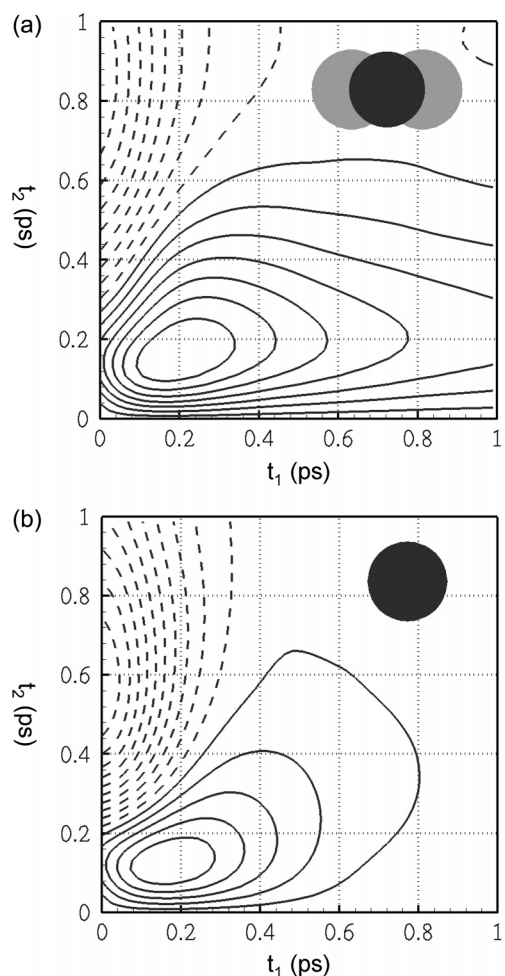
Figure 4. The origin of the nodal lines in the 5th-order Raman spectrum of our solution of CS_2 in liquid Xe. We start by considering the total induced contribution to the TP rotational invariant, Fig. 3(c) (which has a barely visible node in the upper left-hand corner). (a) The total induced contribution to this invariant with the polarizability anisotropy of the CS_2 solute (γ in Eq. (1)) set to zero. (b) The total induced contribution to the invariant when the CS_2 solute has both zero polarizability anisotropy and its C-S distances reduced to 0.0157 Å. The pictures in the upper right hand corners of panels (a) and (b) represent the shape of the solute for each case, correctly drawn to scale.

direct relevance to the spectroscopy, and the isotropy of the potential interactions implies that the orientation cannot even influence the spectrum indirectly by any coupling to the intermolecular translation. Hence, the only difference remaining between neat liquid Xe and our imaginary Xe solution lies in the many-body character of the polarizability in the neat liquid. While the solution polarizability stems from just the coupling of the solute to each of the N solvents,

$$\ddot{\Pi}_{induced} \text{(solution)} = 2 \, \alpha_u \, \alpha_v \sum_{j=1}^{N} \ddot{T}(\mathbf{r}_{0j}),$$

with α_u and α_v the polarizabilities of the CS_2 solute and Xe solvent, respectively, the neat liquid has a contribution from every pair of solvents in the liquid:

$$\ddot{\Pi}_{induced} \text{(neat liquid)} = (\alpha_v)^2 \sum_{\substack{j, k = 1 \\ j \neq k}}^{N} \ddot{T}(\mathbf{r}_{jk}).$$

The response function of the neat liquid will therefore contain cross terms absent in the solution. It is these cross terms that must be responsible for suppressing the nodal lines -- which we would predict would otherwise appear even in an atomic liquid.

Concluding Remarks

The somewhat specialized systems we have chosen to investigate via two-dimensional Raman spectroscopy seems to have presented us with useful case studies. Because we were able to compare two closely related liquids, a single-component atomic liquid and the same liquid with a dilute molecular solute, we found that we were able to draw a number of conclusions about the features of this spectroscopy that directly reflect the anisotropy of molecules. In particular, we now know that it is at least possible to attach a microscopic significance to the signals generated under different polarization conditions.

The key ingredients in this analysis were the rotational invariants that combine to make up the experimental signals under various polarization conditions. For example, we noted that the triple-trace invariant is entirely the result of the time-evolving interaction-induced part of the many-body polarizability. Both our atomic liquid and our solution have such interaction-induced parts but (at our level of treatment of the polarizability) the triple trace vanishes identically for a neat atomic liquid,[46] so this invariant is explicitly molecular. However it is difficult to say more based on these calculations alone. For our solution the dynamics seen by this invariant could arise from either the center-of-mass translation or the solute reorientation (or both). It is interesting to note, though, that while the invariant needs a nonspherical molecular shape to be nonvanishing, it does not need the molecule to rotate. The anisotropy of the molecular polarizability could give rise to a signal by a kind of "heterodyned" process, merely amplifying and making visible the translational dynamics.

By way of contrast, the triple-product invariant, the invariant at the other end of the scale, lent itself much more easily to interpretation. We saw that while this invariant could have had contributions from the time evolutions of both the single-molecule and the interaction-induced polarizabilities, the former was noticeably larger in our solution example. As a result, we can be fairly confident that this invariant mostly tracks the reorientational dynamics of our solute in the solution case.

This last feature points out another key feature of our analysis. The comparison between neat Xe liquid and the Xe solution is a comparison between a system with many identically polarizable species and a system with one, uniquely large polarizability. Having such an inhomogeneous set of polarizabilities significantly decouples the response functions

of the solution, permitting the single-molecule terms to dominate whenever they are symmetry allowed. More than that though, this decoupling may be what allows us to see some of the nodal lines and to see what might be independent-mode behavior, both of which stand in marked contrast to the results for neat liquid Xe.

Understanding the nodes was, of course, one of the main goals of this work. However what the evidence in this paper suggests is that there may not much to understand. Nodes seem to appear and disappear with little systematic regularity: They show up in the original rotational invariants and in the combinations of invariants that correspond to experimental polarization conditions. They can arise from either the single-molecule part of the polarizability or the interaction-induced part. They can show up in a molecular liquid or an atomic mixture. If there is any physical significance to the presence (or more likely to the absence) of nodal lines beyond their being a sensitive measure of the similarity of two different studies, it is a significance yet to be uncovered.

A more promising avenue for investigation, perhaps, is to delve more deeply into the specific dynamical origins of each of the rotational invariants. Straightforward molecular dynamics can only take us so far in associating specific signals with specific kinds of molecular motion. It cannot tell us, for example whether rotational and librational motions differ noticeably from translation in their 5th-order Raman signatures. Nor can it tell us whether the spectrum is really looking at the anharmonicity inherent in the liquid dynamics or the presence of nonlinearity in the coupling of that dynamics to the experimental signal.[3,18,22-24,47] To pursue these questions we have carried out instantaneous-normal-mode analyses[16,18] on the two-dimensional Raman spectra of this same CS_2/Xe solution. The findings from these studies will be presented in a subsequent paper.[35]

References

1. Tanimura, Y.; Mukamel, S. *J. Chem. Phys.* **1993**, *99*, 9496.
2. Mukamel, S.; Piryatinski, A.; Chernyak, V. *Acc. Chem. Res.* **1999**, *32*, 145.
3. In *Ultrafast Infrared and Raman Spectroscopy*; Fleming, G. R.; Blank, D. A.; Cho, M.; Tokmakoff, A.; Fayer, M. D., Eds.; Marcel Dekker: New York, U. S. A., 2001.
4. Steffen, T.; Fourkas, J. T.; Duppen, K. *J. Chem. Phys.* **1996**, *105*, 7364.
5. Blank, D. A.; Kaufman, L. J.; Fleming, G. R. *J. Chem. Phys.* **2000**, *113*, 771.
6. Kaufman, L. J.; Blank, D. A.; Fleming, G. R. *J. Chem. Phys.* **2001**, *114*, 2312.
7. Kaufman, L. J.; Heo, J.; Fleming, G. R.; Sung, J.; Cho, M. *Chem. Phys.* **2001**, *266*, 251.
8. Kaufman, L. J.; Heo, J. Y.; Ziegler, L. D.; Fleming, G. R. *Phys. Rev. Lett.* **2002**, *88*, 207402.
9. Astinov, V.; Kubarych, K. J.; Milne, C. J.; Miller, R. J. Dwayne *Opt. Lett.* **2000**, *25*, 853; *Chem. Phys. Lett.* **2000**, *327*, 334.
10. Kubarych, K. J.; Milne, C. J.; Lin, S.; Miller, R. J. Dwayne *Appl. Phys. B − Laser Opt.* **2002**, *74*, 107; *J. Chem. Phys.* **2002**, *116*, 2016.
11. Golonzka, O.; Demirdöven, N.; Tokmakoff, A. (preprint); Golonzka, O.; Demirdöven, N.; Khalil, M.; Tokmakoff, A. *J. Chem. Phys.* **2000**, *113*, 9893.
12. Frenkel, D.; McTague, J. P. *J. Chem. Phys.* **1980**, *72*, 2801.
13. Geiger, L. C.; Ladanyi, B. M. *J. Chem. Phys.* **1987**, *87*, 191; **1988**, *89*, 6588.
14. Geiger, L. C.; Ladanyi, B. M. *Chem. Phys. Lett.* **1989**, *159*, 413.
15. Stassen, H.; Steele, W. A. *J. Chem. Phys.* **1999**, *110*, 7382.
16. Ma, A.; Stratt, R. M. *Phys. Rev. Lett.* **2000**, *85*, 1004.
17. Ma, A.; Stratt, R. M. *J. Chem. Phys.* **2002**, *116*, 4962.
18. Ma, A.; Stratt, R. M. *J. Chem. Phys.* **2002**, *116*, 4972.
19. Denny, R. A.; Reichman, D. R. *Phys. Rev. E* **2001**, *63*, 065101; *J. Chem. Phys.* **2002**, *116*, 1987.
20. Cao, J. S.; Yang, S. L.; Wu, J. L. *J. Chem. Phys.* **2002**, *116*, 3760.
21. Saito, S.; Ohmine, I. *J. Chem. Phys.* **1998**, *108*, 240.
22. Okumura, K.; Tanimura, Y. *J. Chem. Phys.* **1997**, *107*, 2267.
23. Tokmakoff, A.; Lang, M. J.; Jordanides, X. J.; Fleming, G. R. *Chem. Phys.* **1998**, *233*, 231.
24. Steffen, T.; Duppen, K. *Chem. Phys. Lett.* **1998**, *290*, 229.
25. Similar ideas motivated the optical-Kerr-effect experiments that have been carried out on solutions of CS_2 in alkanes. See Steffen, T; Meinders, N. A. C. M.; Duppen, K. *J. Phys. Chem. A* **1998**, *102*, 4213; McMorrow, D.; Thantu, N.; Melinger, J. S.; Kim, S. K.; Lotshaw, W. T. *J. Phys. Chem.* **1996**, *100*, 10389.
26. Gray, C. G.; Gubbins, K. E. *Theory of Molecular Fluids*, Vol. 1; Clarendon Press: Oxford, U. K., 1984; p 577.
27. Kim, J.; Keyes, T. *Phys. Rev. E* **2002**, *65*, 061102.
28. Murry, R. L.; Fourkas, J. T. *J. Chem. Phys.* **1997**, *107*, 9726.
29. Murry, R. L.; Fourkas, J. T.; Keyes, T. *J. Chem. Phys.* **1998**, *109*, 7913.
30. At the level of our treatment, the spectrum of pure liquid Xe has no qualitative dependence on polarization. Including higher order terms in the dipole-induced-dipole series would introduce a finite, though small, dependence. See Ref. 17.
31. Saito, S.; Ohmine, I. *Phys. Rev. Lett.* **2002**, *88*, 207401.
32. Jansen, T. I. C.; Snijders, J. G.; Duppen, K. *J. Chem. Phys.* **2000**, *113*, 307; **2001**, *114*, 10910.
33. Steffen, T.; Duppen, K. *Chem. Phys. Lett.* **1997**, *273*, 47.
34. Steffen, T.; Duppen, K. *Chem. Phys.* **1998**, *233*, 267.
35. Ma, A.; Stratt, R. M. *J. Chem. Phys.* **2003** in press.
36. Allen, M. P.; Tildesley, D. J. *Computer Simulation of Liquids*; Clarendon Press: Oxford, U. K., 1987; pp 20-22.
37. Sherwood, A. E.; Prausnitz, J. M. *J. Chem. Phys.* **1964**, *41*, 429.
38. Fincham, D. *Molecular Simulation* **1993**, *11*, 79.
39. Ref. 36, chap. 3.
40. Barojas, J.; Levesque, D.; Quentrec, B. *Phys. Rev. A* **1973**, *7*, 1092.
41. Andersen, H. C. *J. Comp. Phys.* **1983**, *52*, 24.
42. Deng, Y., *Ph. D. Thesis*; Brown University: 2002.
43. Ref. 36, p 171.
44. Eqs. (7) and (8) imply that any constant portion of the many-body polarizability will have an identically zero contribution to the 5-th order signal
45. Note that this conclusion is specific to our system, which has a molecular polarizability larger in magnitude than any of the induced polarizabilities. One can probably not make a similar statement for neat liquid CS_2.
46. The dipole-dipole tensors in Eq. (4) have zero trace. See Ref. 17.
47. Chernyak, V.; Mukamel, S. *J. Chem. Phys.* **1998**, *108*, 5812.